Available online at www.sciencedirect.com
SCIENCE DIRECT®
European Journal of Pharmaceutical Sciences 22 (2004) 43–53
EUROPEAN JOURNAL OF PHARMACEUTICAL SCIENCES
www.elsevier.com/locate/ejps

Design, synthesis, and computational affinity prediction of ester soft drugs as inhibitors of dihydrofolate reductase from *Pneumocystis carinii*

Malin Graffner-Nordberg [a,1], Karin Kolmodin [b,2], Johan Åqvist [b], Sherry F. Queener [c], Anders Hallberg [a,*]

[a] *Department of Medicinal Chemistry, Uppsala Biomedical Center, Uppsala University, Box 574, SE-751 23 Uppsala, Sweden*
[b] *Department of Cell and Molecular Biology, Uppsala Biomedical Center, Uppsala University, Box 596, SE-751 24 Uppsala, Sweden*
[c] *Department of Pharmacology and Toxicology, School of Medicine, Indiana University, Indianapolis, IN 46202, USA*

Received 13 October 2003; received in revised form 2 February 2004; accepted 17 February 2004

Abstract

A series of dihydrofolate reductase (DHFR) inhibitors, where the methylenamino-bridge of non-classical inhibitors was replaced with an ester function, have been prepared as potential soft drugs intended for inhalation against *Pneumocystis carinii* pneumonia (PCP). Several of the new ester-based inhibitors that should serve as good substrates for the ubiquitous esterases and possibly constitute safer alternatives to metabolically stable DHFR inhibitors administered orally, were found to be potent inhibitors of *P. carinii* DHFR (pcDHFR). Although the objectives of the present program is to achieve a favorable toxicity profile by applying the soft drug concept, a high preference for inhibition of the fungal DHFR versus the mammalian DHFR is still desirable to suppress host toxicity at the site of administration. Compounds with a slight preference for the fungal enzyme were identified. The selection of the target compounds for synthesis was partly guided by an automated docking and scoring procedure as well as molecular dynamics simulations. The modest selectivity of the synthesized inhibitors was reasonably well predicted, although a correct ranking of the relative affinities was not successful in all cases.

Keywords: Dihydrofolate reductase; Soft drug; Molecular dynamics; *Pneumocystis carinii*

1. Introduction

The enhanced use of prophylaxis and highly active antiretroviral therapy (HAART) in patients known to be at risk for developing *Pneumocystis carinii* pneumonia (PCP), has markedly decreased the incidence of PCP in patients with AIDS (Schliep and Yarrish, 1999; Kaplan et al., 2000; Arozullah et al., 2000). PCP is a serious pulmonary disease caused by the fungus *P. carinii* and is the major cause of mortality among patients suffering from AIDS (Kovacs et al., 1984; Mills, 1986; Glatt and Chirgwin, 1990; McKenzie et al., 1991; Miller and Mitchell, 1995). Current treatment of PCP with trimethoprim (TMP, Fig. 1), a nonclassical inhibitor of dihydrofolate reductase (DHFR), in combination with a sulfonamide (co-trimoxazole) is still the first-line therapy in clinic (Fischl et al., 1988; Walker and Masur, 1994; Miller and Mitchell, 1995; Schliep and Yarrish, 1999). However, most often severe side-effects associated with sulfa drugs lead to discontinuation of therapy (Gordin et al., 1984; Glatt and Chirgwin, 1990; Masur, 1992; Roudier et al., 1994). Attempts have been made to use drugs locally to treat PCP. Thus, inhaled aerosolized pentamidine is used for prophylaxis (Golden et al., 1989; Leoung et al., 1990; Monk and Benfield, 1990; Hirschel et al., 1991), although this route of administration is inadequate for treatment of the active infection. Systemic

* Corresponding author. Tel.: +46-18-471-4284; fax: +46-18-471-4976.
E-mail address: anders.hallberg@farmkemi.uu.se (A. Hallberg).
[1] Present address: Department of Medicinal Chemistry, Biovitrum AB, SE-751 82 Uppsala, Sweden.
[2] Present address: EST Chemical Computing, AstraZeneca R&D Mölndal, SE-431 83 Molndal, Sweden.

0928-0987/$ – see front matter © 2004 Elsevier B.V. All rights reserved.
doi:10.1016/j.ejps.2004.02.004

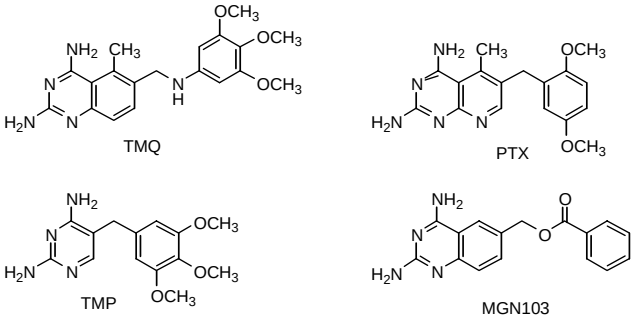

Fig. 1. Chemical structures of compounds TMQ, PTX, TMP and MGN103.

administration of pentamidine exhibits a considerable toxicity (Pearson and Hewlett, 1985; Monk and Benfield, 1990; Walker and Masur, 1994; Schliep and Yarrish, 1999). Trimetrexate (TMQ, Fig. 1) (Elslager and Davoll, 1974; Elslager et al., 1983) and piritrexim (PTX, Fig. 1) (Grivsky et al., 1980), are two new lipophilic agents originally developed as anticancer agents (Bertino et al., 1979; Duch et al., 1982; Weir et al., 1982; Lin et al., 1987; Kovacs et al., 1988). Recently, both drugs, TMQ in particular, have found a place as second-line therapy in moderate to severe PCP (Anonymous, 1994). Although TMQ and PTX are potent inhibitors of DHFR from *P. carinii*, they are not selective and inhibit the mammalian enzyme even more efficiently (Allegra et al., 1987b; Broughton and Queener, 1991). The clinical use of TMQ and PTX is therefore limited as a result of their systemic host toxicity and an expensive co-therapy with the rescue agent leucovorin (5-formyl-tetrahydrofolate) is required (Allegra et al., 1987a,b; Falloon et al., 1990; Sattler et al., 1990; Masur et al., 1993). Consequently, efforts focus on finding more selective as well as more potent antifolates.

The soft drug concept could serve as a new strategy in the search for safer DHFR inhibitors with potential use in the therapy against PCP. Soft drugs are active isosteric–isoelectronic analogues of lead compounds that are deactivated in a predictable and controllable way after exerting their biological effects (Bodor and Buchwald, 2000). These drugs are intended to undergo a fast metabolism to inactive and non-toxic metabolites. Soft drugs are often used for local treatment and are, in general, administered near the site of action (Bodor and Buchwald, 2000). The concept has successfully been utilized, for example, in the design of the recently launched inhaled anti-asthma glucocorticosteroid budesonide (Clissold and Heel, 1984) that, essentially, is devoid of systemic side effects in man due to its rapid first pass metabolism in the liver (Johansson et al., 1982). Furthermore, in an initial report, we recently demonstrated with one example that a lipophilic ester acting as a DHFR inhibitor was rapidly inactivated after oral or intravenous administration in rat (Graffner-Nordberg et al., 2000). We believe that the application of the soft drug concept should allow for identification of new DHFR inhibitors suitable for inhalation against PCP.

We have now prepared a series of lipophilic esters anticipated to serve as substrates for the ubiquitously distributed esterases. We herein report the impact of various aromatic scaffolds on the inhibition of DHFR from *P. carinii* DHFR (pcDHFR) and the corresponding mammalian enzyme (rlDHFR). The selection of the target compounds for synthesis was partly guided by molecular dynamics simulation and the docking program AutoDock 3.0 (Morris et al., 1998).

2. Materials and methods

2.1. Chemistry: general procedures

^{1}H and ^{13}C NMR spectra were recorded on a JEOL JNM-EX270 spectrometer at 270 and 67.8 MHz, respectively, and a JEOL JNM-EX400 spectrometer at 400 and 100 MHz, respectively. Thin-layer chromatography (TLC) was performed by using aluminium sheets precoated with silica gel 60 F_{254} (0.2 mm) type E; Merck. Chromatographic spots were visualized by UV light. Column chromatography was conducted on silica gel 60 (0.040–0.063 mm; Merck), unless otherwise noted. Melting points (uncorrected) were determined in open glass capillaries on an Electrothermal apparatus. The Quest 210 organic synthesizer (Argonaut Technologies) was used in the syntheses of **3**–**4**, **6**–**8**, **12**, **14**–**15**. In the syntheses of **10** and **11** microwave heating was performed in a Smith Synthesizer^{TM} single mode microwave cavity producing continuous irradiation at 2450 MHz (Personal Chemistry AB, Uppsala, Sweden). The syntheses were performed in heavy-walled glass Smith Process Vials sealed with aluminum crimp caps fitted with a silicon septum. The inner diameter of the vial filled to the height of 2 cm was 1.3 cm. Reaction mixtures were stirred with a magnetic stir bar during the irradiation. The temperature, pressure and irradiation power was monitored during the course of the reaction. The average pressure during the reaction was 3–4 bar. After completed irradiation, the reaction tube was cooled with high-pressure air until the temperature had fallen below 39 °C (ca. 2 min). The microwave irradiations were performed under controlled conditions that make the procedure highly safe, reliable and reproducible. Single mode irradiation with monitoring of temperature, pressure and irradiation power versus time was used throughout. The reaction temperature was kept constant throughout the reaction in the single mode cavity by an automatic power control. Caution! When carrying out reactions with microwave irradiation in closed vessels, extra caution is advisable. In addition to the high pressure generated by the vapor pressure of volatile components, the metal catalysts might precipitate and cause a “thermal runaway”, increasing the pressure further. Therefore, the use of special heavy-walled process vials is highly recommended. SpeedVac® Plus SC250DDA (Savant) was used in the evaporations of DMF. The elemental analyses were performed by Mikro Kemi AB, Uppsala, Sweden and were within ±0.4% of the calculated values. The synthesis of

2,4-diamino-6-bromomethylquinazoline has been described elsewhere (Graffner-Nordberg et al., 2000). All commercial chemicals were used without further purification.

2.1.1. (2,4-Diaminoquinazoline-6-yl)methyl 1-naphthoate (1)

A solution of 2,4-diamino-6-bromomethylquinazoline (0.53 mmol) in anhydrous DMF (2 ml) was added dropwise to a mixture of 1-naphthoic acid (272 mg, 1.58 mmol), and potassium carbonate (218 mg, 1.58 mmol) in DMF (total amount: 5 ml). The reaction mixture was stirred under nitrogen at room temperature for 2 days before the crude product was evaporated under reduced pressure on a small portion of silica gel. The silica plug was loaded on the top of a silica column, previously packed with dichloromethane, and the crude ester was purified by repeated flash chromatography [CH_2Cl_2:MeOH + NH_3 (19:1 yielding 80 mg (44% over two steps): ^{1}H NMR (DMF-d_6) δ 8.88–8.84 (app d, 1H, Ar*H*), 8.26 (d, J = 1.98 Hz, 1H, *H*-5), 8.22–8.18 (m, 2H, Ar*H*), 8.05–8.02 (m, 1H, Ar*H*), 7.71 (dd, J = 8.58, 1.98 Hz, 1H, *H*-7), 7.68–7.55 (m, 3H, Ar*H*), 7.46 (br s, 2H, NH_2), 7.28 (d, J = 8.58 Hz, 1H, *H*-8), 6.12 (br s, 2H, NH_2), 5.45 (s, 2H, CH_2); ^{13}C NMR (DMF-d_6) δ 167.61, 163.80, 162.90, 153.92, 134.60, 134.19, 133.78, 131.71, 130.90, 129.48, 128.51, 128.44, 127.63, 127.07, 126.01, 125.76, 125.57, 124.81, 111.01, 67.64. Anal. ($C_{20}H_{16}N_4O_2 \cdot 0.4H_2O$) C, H, N.

2.1.2. (2,4-Diaminoquinazoline-6-yl)methyl 2-naphthoate (2)

Compound **2** was prepared as described for **1** using 2-naphthoic acid (272 mg, 1.58 mmol). The reaction was allowed to proceed for 2 days before it was filtered and worked-up as described above for **1** yielding 60 mg (33% over two steps): ^{1}H NMR (DMF-d_6) δ 8.68 (app s, 1H, Ar*H*), 8.24 (d, J = 1.65 Hz, 1H, *H*-5), 8.14–8.11 (m, 1H, Ar*H*), 8.00–7.98 (m, 2H, Ar*H*), 7.70–7.57 (m, 4H, *H*-7, Ar*H*), 7.45 (br s, 2H, NH_2), 7.27 (d, J = 8.58 Hz, 1H, *H*-8), 6.11 (br s, 2H, NH_2), 5.41 (s, 2H, CH_2); ^{13}C NMR (DMF-d_6) δ 166.73, 163.80, 162.90, 153.88, 136.22, 133.63, 133.20, 131.46, 130.08, 129.27, 129.09, 128.46, 128.14, 127.67, 125.75, 125.66, 124.62, 111.00, 67.55 (one carbon missing). Anal. ($C_{20}H_{16}N_4O_2 \cdot 0.25H_2O$) C, H, N.

2.1.3. (2,4-Diaminoquinazoline-6-yl)methyl 9-phenanthrenecarboxylate (3)

Compound **3** was prepared using the Quest 210 organic synthesizer starting with 2,4-diamino-6-bromomethylquinazoline (0.53 mmol), 9′-phenanthrenecarboxylic acid (351 mg, 1.58 mmol), and potassium carbonate (218 mg, 1.58 mmol) in DMF (total amount: 5 ml). The reaction was allowed to proceed for 2 days before it was filtered and rinsed with DMF. A small portion of silica gel was added to the reaction mixture and the solvent was evaporated using SpeedVac®. The silica plug was loaded on the top of a silica column, previously packed with dichloromethane, and the crude ester was purified as described for compound **1** yielding 34 mg (22% over two steps): ^{1}H NMR (DMSO-d_6) δ 8.95–8.87 (m, 3H, Ar*H*), 8.54 (s, 1H, Ar*H*), 8.19–8.16 (m, 3H, Ar*H*), 7.56–7.68 (m, 4H, *H*-7 + Ar*H*), 7.35 (br s, 2H, NH_2), 7.25 (d, J = 8.58 Hz, 1H, *H*-8), 6.07 (br s, 2H, NH_2), 5.46 (s, 2H, CH_2); ^{13}C NMR (DMSO-d_6) δ 166.84, 162.50, 161.13, 152.67, 133.23, 131.72, 131.40, 131.21, 130.05, 129.54, 129.45, 128.18, 127.60, 127.51, 127.35, 127.08, 125.99, 124.60, 124.32, 123.47, 123.00, 109.98, 67.07 (one carbon missing). Anal. ($C_{24}H_{18}N_4O_2 \cdot 1H_2O$) C, H, N.

2.1.4. (2,4-Diaminoquinazoline-6-yl)methyl 9-anthracencarboxylate (4)

Compound **4** was prepared as described for **3** using the Quest 210 organic synthesizer starting with 9-anthracenecarboxylic acid (351 mg, 1.58 mmol). The reaction was allowed to proceed for 2 days before it was filtered and worked-up as described above for **3** yielding 50 mg (24% over two steps): ^{1}H NMR (DMSO-d_6) δ 8.95–8.87 (m, 3H, Ar*H*), 8.54 (s, 1H, Ar*H*), 8.19–8.16 (m, 3H, Ar*H*), 7.56–7.68 (m, 4H, *H*-7 + Ar*H*), 7.35 (br s, 2H, NH_2), 7.25 (d, J = 8.58 Hz, 1H, *H*-8), 6.07 (br s, 2H, NH_2), 5.46 (s, 2H, CH_2); ^{13}C NMR (DMSO-d_6) δ 168.62, 162.47, 161.12, 152.70, 133.56, 130.40, 129.21, 128.67 (2C), 127.42 (3C), 126.61, 125.78 (2C), 124.94, 124.54, 124.43 (2C), 109.90, 67.78 (three carbons missing). Anal. ($C_{24}H_{18}N_4O_2 \cdot 0.25H_2O$) C, H, N.

2.1.5. (2,4-Diaminoquinazoline-6-yl)methyl diphenylacetate (5)

Compound **5** was prepared as described for **1** using diphenylacetic acid (335 mg, 1.58 mmol). The reaction was allowed to proceed for 2 days before it was filtered and worked-up as described above for **1** yielding 72 mg (36% over two steps): ^{1}H NMR (DMF-d_6) δ 8.08 (d, J = 1.65 Hz, 1H, *H*-5), 7.45 (dd, J = 8.58, 1.98 Hz, 1H, *H*-7), 7.41 (br s, 2H, NH_2), 7.37–7.19 (m, 10H, Ar*H*), 7.19 (d, J = 8.58 Hz, 1H, *H*-8), 6.16 (br s, 2H, NH_2), 5.25 (s, 1H, C*H*), 5.17 (s, 2H, CH_2); ^{13}C NMR (DMF-d_6) δ 172.79, 163.73, 153.51, 140.07 (2C), 133.71, 129.25 (2C), 129.18 (2C), 128.21, 127.78 (2C), 125.44 (2C), 124.87, 110.78, 67.55, 56.93 (2C) (three carbons missing). Anal. ($C_{23}H_{20}N_4O_2$) C, H, N.

2.1.6. (2,4-Diaminoquinazoline-6-yl)methyl 2′-benzylbenzoate (6)

Compound **6** was prepared as described for **3** using the Quest 210 organic synthesizer starting with 2-benzylbenzoic acid (334 mg, 1.58 mmol). The reaction was allowed to proceed for 2 days before it was filtered and worked-up as described above for **3** yielding 53 mg (26% over two steps): ^{1}H NMR (DMSO-d_6) δ 8.06 (d, J = 1.65 Hz, 1H, *H*-5), 7.83–7.80 (m, 1H, Ar*H*), 7.54–7.04 (m, 12H, NH_2 + Ar*H*), 6.04 (br s, 2H, NH_2), 5.24 (s, 2H, CH_2), 4.28 (s, 2H, CH_2); ^{13}C NMR (DMSO-d_6) δ 166.81, 162.26, 160.83, 152.27, 141.39, 140.59, 132.96, 132.01, 131.32, 130.03, 129.51, 128.36 (2C), 128.05 (2C), 126.85, 126.31, 125.66,

124.28, 124.06, 109.65, 64.48 (one carbon missing). Anal. ($C_{23}H_{20}N_4O_2$) C, H, N.

2.1.7. (2,4-Diaminoquinazoline-6-yl)methyl 2′-phenylbenzoate (7)

Compound **7** was prepared as described for **3** using the Quest 210 organic synthesizer starting with 2-phenylbenzoic acid (313 mg, 1.58 mmol). The reaction was allowed to proceed for 2 days before it was worked-up as described above for **3** yielding 47 mg (24% over two steps): ^{1}H NMR (DMSO-d$_6$) δ 7.90 (app s, 1H, *H*-5), 7.78–7.09 (m, 13H, Ar*H*), 6.04 (br s, 2H, NH_2), 5.05 (s, 2H, CH_2); ^{13}C NMR (DMSO-d$_6$) δ 168.00, 162.39, 162.11, 161.68, 161.05, 152.55, 141.23, 140.35, 132.87, 131.45, 130.93, 130.48, 129.28, 128.38, 128.13, 127.43, 127.20, 126.46, 124.32, 124.09, 109.70, 66.81. Anal. ($C_{22}H_{18}N_4O_2\cdot0.25H_2O$) C, H, N.

2.1.8. (2,4-Diaminoquinazoline-6-yl)methyl 4′-phenylbenzoate (8)

Compound **8** was prepared as described for **3** using the Quest 210 organic synthesizer starting with 4-phenylbenzoic acid (313 mg, 1.58 mmol). The reaction was interrupted after 2 days and further worked-up as described above for **3** yielding 25 mg (13% over two steps): ^{1}H NMR (DMSO-d$_6$) δ 8.11–7.21 (m, 14H, Ar*H*), 6.12 (br s, 2H, NH_2), 5.34 (s, 2H, CH_2); ^{13}C NMR (DMSO-d$_6$) δ 165.48, 162.46, 160.81, 152.09, 144.76, 138.80, 133.03, 129.94, 129.11, 128.46, 128.21, 128.14, 127.30, 126.99, 124.28, 124.03, 109.89, 66.62 (four carbons missing). Anal. ($C_{22}H_{18}N_4O_2\cdot0.75H_2O$) C, H, N.

2.1.9. (2,4-Diaminoquinazoline-6-yl)methyl 3′-iodobenzoate (9)

Compound **9** was prepared as described for **1** starting with 2,4-diamino-6-bromomethylquinazoline (2.52 mmol), 3-iodobenzoic acid (1.87 g, 7.57 mmol), and potassium carbonate (1.04 g, 7.57 mmol) in DMF (total amount: 20 ml). The reaction was allowed to proceed for 2 days before it was filtered and worked-up as described above for **1** yielding 441 mg (42% over two steps). Recrystallization from methanol afforded 360 mg (34%) as white needles: ^{1}H NMR (DMSO-d$_6$) δ 8.25 (dd, J = 1.32, 1.32 Hz, 1H, Ar*H*), 8.08 (d, J = 1.65 Hz, 1H, *H*-5), 8.04–7.98 (m, 2H, Ar*H*), 7.59 (dd, J = 8.58, 1.65 Hz, 1H, *H*-7), 7.32 (br s, 2H, NH_2), 7.34 (dd, J = 7.92, 7.92 Hz, 1H, Ar*H*), 7.20 (d, J = 8.58 Hz, 1H, *H*-8), 6.05 (br s, 2H, NH_2), 5.32 (s, 2H, CH_2); ^{13}C NMR (DMSO-d$_6$) δ 164.00, 162.12, 160.77, 152.34, 141.56, 137.03, 132.65, 131.34, 130.64, 128.28, 126.49, 124.22, 123.76, 109.58, 94.56, 66.69. Anal. ($C_{16}H_{13}IN_4O_2$) C, H, N.

2.1.10. (2,4-Diaminoquinazoline-6-yl)methyl 3′-phenylbenzoate (10)

A heavy-walled glass Smith Process Vial sealed with aluminum crimp caps fitted with a silicon septum was charged with compound **9** (50 mg, 0.12 mmol) in DMF (800 μl), phenylboronic acid (72.5 mg, 0.59 mmol) in DMF (200 μl), $PdCl_2(PPh_3)_2$ (0.8 mg, 1.2 mmol), and 2 M Na_2CO_3 (150 μl), in 2 ml of DME:H_2O:EtOH (7:3:2). The reaction mixture was exposed to microwave irradiation for 120 s at 150 °C. The mixture was filtered through a syringe equipped with a Titan® filter (pore size 0.45 μm). A small portion of silica gel was added to the solution. The solvent was evaporated using SpeedVac®. Purifications were conducted using flash chromatography as described for compound **1** finally yielding 15 mg (34%) of the target molecule: ^{1}H NMR (DMSO-d$_6$) δ 8.20–8.18 (m, 1H, Ar*H*), 8.10 (d, J = 1.65 Hz, 1H, *H*-5), 8.00–7.93 (m, 2H, Ar*H*), 7.70–7.37 (m, 9H, Ar*H* + NH_2), 7.22 (d, J = 8.58 Hz, 1H, *H*-8), 6.07 (br s, 2H, NH_2), 5.36 (s, 2H, CH_2); ^{13}C NMR (DMSO-d$_6$) δ 165.98, 162.82, 161.22, 152.54, 141.08, 139.41, 133.46, 132.04, 132.73, 129.94, 129.49 (2C), 128.61, 128.38, 127.68, 127.55, 127.19 (2C), 124.71, 124.37, 110.21, 67.09. Anal. ($C_{22}H_{18}N_4O_2\cdot0.25H_2O$) C, H, N.

2.1.11. (2,4-Diaminoquinazoline-6-yl)methyl [2′,6′-dimethoxy]-3′-phenylbenzoate (11)

Compound **11** was performed as for compound **10** using 2,6-dimethoxyphenylboronic acid (108 mg, 0.59 mmol). Work-up was conducted as described for the synthesis of **10** providing 20 mg (39%) of the target molecule: ^{1}H NMR (DMSO-d$_6$) δ 8.09 (app s, 1H, *H*-5), 7.92–7.89 (m, 1H, Ar*H*), 7.78 (m, 1H, Ar*H*), 7.60 (dd, J = 8.58, 1.98 Hz, 1H, *H*-7), 7.55–7.46 (m, 2H, Ar*H*), 7.35–7.30 (m, 3H, Ar*H* + NH_2), 7.22 (d, J = 8.58 Hz, 1H, *H*-8), 6.75 (d, J = 8.58 Hz, 1H, *H*-8), 6.06 (br s, 2H, NH_2), 5.32 (s, 2H, CH_2) 3.64 (s, 6H, CH_3); ^{13}C NMR (DMSO-d$_6$) δ 166.11, 162.80, 161.20, 157.32, 152.52, 136.21, 135.08, 133.50, 131.77, 129.89, 129.54, 128.54, 127.85, 127.71, 124.67, 124.46, 117.61, 110.19, 104.69, 66.93, 56.04 (2C) (two carbons missing). Anal. ($C_{24}H_{22}N_4O_4\cdot2H_2O$) C, H; N: calcd, 12.0; found, 11.3.

2.1.12. (2,4-Diaminoquinazoline-6-yl)methyl 3′,5′-dimethylbenzoate (12)

Compound **12** was prepared as described for **3** using the Quest 210 organic synthesizer starting with 3,5-dimethylbenzoic acid (237 mg, 1.58 mmol). The reaction was allowed to proceed for 2 days before it was filtered and worked-up as described above for **3** yielding 32 mg (19% over two steps): ^{1}H NMR (DMSO-d$_6$) δ 8.08 (d, J = 1.65 Hz, 1H, *H*-5), 7.32 (br s, 2H, NH_2), 7.20 (d, J = 8.58 Hz, 1H, *H*-8), 7.28 (s, 1H, Ar*H*), 7.59–7.56 (m, 3H, NH_2 + Ar*H*), 6.06 (br s, 2H, NH_2), 5.29 (s, 2H, CH_2), 3.36 (s, 6H); ^{13}C NMR (DMSO-d$_6$) δ 165.87, 162.44, 161.09, 152.63, 138.02 (2C), 134.74, 133.08, 129.61, 127.10, 126.85 (2C), 124.57, 124.19, 109.90, 66.58, 20.68 (2C). Anal. ($C_{18}H_{18}N_4O_2\cdot1.75H_2O$) C, H; N: calcd, 16.12; found, 15.50.

*2.1.13. (2,4-Diaminoquinazoline-6-yl)methyl 2-thiophenecarboxylate (**13**)*

Compound **13** was prepared as described for **1** using 2-thiophenecarboxylic acid (202 mg, 1.58 mmol). The reaction was allowed to proceed for 2 days before it was filtered and worked-up as described above for **1** yielding 63 mg (40% over two steps): ^{1}H NMR (DMF-d$_6$) δ 8.28 (d, J = 1.65 Hz, 1H, *H*-5), 7.98 (br s, 2H, N*H*$_2$), 7.96 (m, 1H, Ar*H*), 7.85–7.83 (m, 1H, Ar*H*), 7.72 (dd, J = 8.58, 1.98 Hz, 1H, *H*-7), 7.36 (d, J = 8.58 Hz, 1H, *H*-8), 7.24–7.21 (m, 1H, Ar*H*), 6.81 (br s, 2H, N*H*$_2$), 5.35 (s, 2H, C*H*$_2$); ^{13}C NMR (DMF-d$_6$) δ 163.99, 160.37, 149.38, 134.54 (2C), 129.85, 128.99, 125.03, 123.15, 110.71, 67.21 (three carbons missing). Anal. ($C_{14}H_{12}N_4O_2S{\cdot}0.5H_2O$) C, H, N.

*2.1.14. (2,4-Diaminoquinazoline-6-yl)methyl 3-thiophenecarboxylate (**14**)*

Compound **14** was prepared as described for **3** using the Quest 210 organic synthesizer starting with 3′-thiophenecarboxylic acid (202 mg, 1.58 mmol). The silica plug was loaded on the top of a silica column, previously packed with dichloromethane, and the crude ester was purified as described for compound **1** yielding 34 mg (22% over two steps): ^{1}H NMR (DMSO-d$_6$) δ 8.40–8.38 (m, 1H, Ar*H*), 8.06 (d, J = 1.65 Hz, 1H, *H*-5), 7.67–7.64 (m, 1H, Ar*H*), 7.56 (dd, J = 8.58, 1.98 Hz, 1H, *H*-7), 7.50–7.48 (m, 1H, Ar*H*), 7.31 (br s, 2H, N*H*$_2$), 7.20 (d, J = 8.58 Hz, 1H, *H*-8), 6.05 (br s, 2H, N*H*$_2$), 5.26 (s, 2H, C*H*$_2$); ^{13}C NMR (DMSO-d$_6$) δ 162.44, 161.97, 161.06, 152.58, 134.09, 132.92, 132.80, 127.73, 127.49, 127.15, 124.51, 123.90, 109.89, 66.19. Anal. ($C_{14}H_{12}N_4O_2S$) C, H, N.

*2.1.15. (2,4-Diaminoquinazoline-6-yl)methyl 2-furoate (**15**)*

Compound **15** was prepared as described for **3** using the Quest 210 organic synthesizer starting with 2-furoic acid (177 mg, 1.58 mmol). The reaction was allowed to proceed for 2 days before it was filtered and worked-up as described above for **3** yielding 25 mg (17% over two steps): ^{1}H NMR (DMSO-d$_6$) δ 8.40–8.38 (m, 1H, Ar*H*), 8.06 (d, J = 1.65 Hz, 1H, *H*-5), 7.67–7.64 (m, 1H, Ar*H*), 7.56 (dd, J = 8.58, 1.98 Hz, 1H, *H*-7), 7.50–7.48 (m, 1H, Ar*H*), 7.31 (br s, 2H, N*H*$_2$), 7.20 (d, J = 8.58 Hz, 1H, *H*-8), 6.05 (br s, 2H, N*H*$_2$), 5.26 (s, 2H, C*H*$_2$); ^{13}C NMR (DMSO-d$_6$) δ 162.44, 161.97, 161.06, 152.58, 134.09, 132.92, 132.80, 127.73, 127.49, 127.15, 124.51, 123.90, 109.89, 66.19. Anal. ($C_{14}H_{12}N_4O_3{\cdot}0.25H_2O$) C, H, N.

*2.1.16. (2,4-Diaminoquinazoline-6-yl)methyl 3-furoate (**16**)*

Compound **16** was prepared as described for **1** using 2-furoic acid (177 mg, 1.58 mmol). The reaction was allowed to proceed for 2 days before it was filtered and worked-up as described above for **1** yielding 30 mg (20% over two steps): ^{1}H NMR (DMSO-d$_6$) δ 8.05 (d, J = 1.65 Hz, 1H, *H*-5), 7.96–7.95 (m, 1H, Ar*H*), 7.56 (dd, J = 8.58, 1.65 Hz, 1H, *H*-7), 7.35–7.34 (m, 3H, N*H*$_2$ + Ar*H*), 7.20 (d, J = 8.58 Hz, 1H, *H*-8), 6.69–6.67 (m, 1H, Ar*H*), 6.06 (br s, 2H, N*H*$_2$), 5.27 (s, 2H, C*H*$_2$); ^{13}C NMR (DMSO-d$_6$) δ 162.34, 160.81, 157.74, 152.19, 147.61, 143.58, 133.11, 126.84, 124.27, 124.14, 118.61, 112.28, 109.71, 66.22. Anal. ($C_{14}H_{12}N_4O_3{\cdot}0.75H_2O$) C, H, N.

2.2. Molecular dynamics

The linear interaction energy (LIE) method (Åqvist et al., 1994; Marelius et al., 1998c; Graffner-Nordberg et al., 2001) was used to estimate the free energy of binding for a number of inhibitors, docked into the active sites of hDHFR and pcDHFR, respectively, using AutoDock. The complexes were further subjected to molecular dynamics simulations from which the energy averages were calculated. All MD simulations were performed using the software package Q (Marelius et al., 1998b) and the GROMOS87 force field (van Gunsteren and Berendsen, 1987). Non-standard charges of NADPH and the inhibitors were derived as in earlier work (Marelius et al., 1998a).

The starting coordinates for the simulations of DHFR from *P. carinii* were taken from the crystal structure of the ternary complex with the enzyme in complex with NADPH and TMP (PDB entry 1DYR). The structure of human DHFR was the L22Y mutant enzyme in complex with NADPH and methotrexate (PDB entry 1DLS) from which the wild type enzyme was modeled prior to simulation. The protein-inhibitor complex was soaked in an 18 Å spherical grid of SPC water molecules. Water molecules generated closer than 2.4 Å to protein or inhibitor atoms were removed. Ionic groups on the protein within about 10 Å from the inhibitors were included, whereas those far from the active site were modeled as neutral dipolar groups. The net charge of the protein and cofactor was zero. Simulations of the free inhibitors were carried out in water spheres of the same size as the protein simulations. The water molecules were subjected to radial and polarization surface restraints and the local reaction field (LRF) (Lee and Warshel, 1992) was used for handling long range electrostatics. The system was heated to 300 K by increasing the temperature incrementally during a 30 ps equilibration phase keeping the protein atoms restrained to their crystallographic positions. The system was then equilibrated without restraining the protein in the simulation sphere for 50 ps. Data collection was performed at 300 K using a time step of 1.5 fs.

2.3. Docking and scoring

All selected compounds were built and geometry optimized using InsightII (MSI, San Diego). Torsions defining the orientation of the ester linkage and the hydrophobic substituents were flexible in the ligands, while the geometry of the 2,4-diaminoquinazoline moiety was fixed in a planar structure. Partial charges of the proteins were assigned from the GROMOS force field (van Gunsteren and Berendsen, 1987), which also was used in the subsequent molecular dynamics simulations. The partial charges of the ligands were

derived using semi-empirical quantum mechanical calculations (Marelius et al., 1998a). The energy grids were calculated using AutoGrid. The grid consisted of $120 \times 120 \times 120$ grid points with a spacing of 0.20 Å centered at the active site of the protein structures, which had the co-crystallized inhibitors and waters removed. Two crystal structures of hDHFR (1HFR (Cody et al., 1998) and 1DLS (Lewis et al., 1995) modeled from L22Y to wild type) and two of pcDHFR (1DYR (Champness et al., 1994) and 3CD2 (Cody et al., 1999)) were used as models for the target proteins. Trimethoprim, which is the inhibitor found in the structure of pcDHFR (1DYR), was used as a reference compound in order to validate whether the program was able to reproduce the experimental structure of the complex. For each combination of ligand and protein AutoDock was run using 50 Lamarckian genetic algorithm runs (Morris et al., 1998) with 1×10^6 energy evaluations. The remaining parameters used by the genetic algorithm were set to the default values given by AutoDock.

After docking, the resulting structures from each run were sorted into clusters using a 1.0 Å tolerance all-atom root mean square deviation (RMSD) from the lowest energy structure. All high-ranked clusters were visually inspected to make sure that the ligands were docked in a reasonable orientation in the active site. Trimethoprim was docked with a root mean square deviation of 1.5 Å compared to the experimental structure. It was mainly the orientation of the methoxy groups that contributed to this relatively large deviation, but the position of the docked ligand was satisfactorily reproduced (Fig. 2).

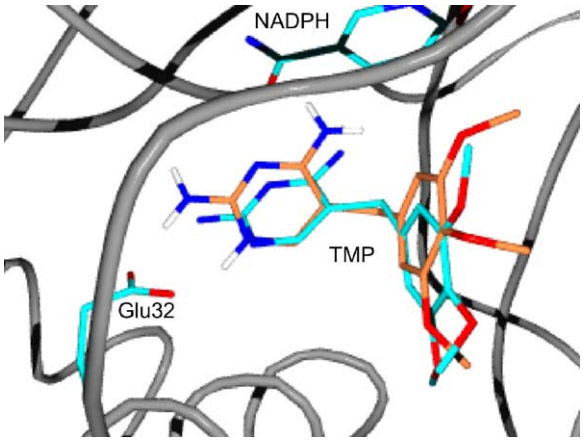

Fig. 2. Trimethoprim in complex with pcDHFR. The position of the inhibitor as determined by X-ray crystallography is shown in cyan (1DYR). In orange, the binding conformation as predicted by AutoDock.

2.4. Inhibition of dihydrofolate reductase

The compounds **1**–**16**, and the reference compounds shown in Fig. 1, were evaluated for their ability to inhibit dihydrofolate reductase from *P. carinii* (pcDHFR) and rat liver (rlDHFR). The methodologies of the assay are described elsewhere (Broughton and Queener, 1991; Chio and Queener, 1993). All results are presented as IC_{50}-values in Table 1. For comparison, the IC_{50}-values for inhibition of *Toxoplasma gondii* DHFR (tgDHFR) and *Mycobacterium avium* (mavDHFR), respectively, are shown.

Table 1
Inhibition concentrations (IC_{50}, μM) of DHFR from *P. carinii*, *T. gondii*, and rat liver and selectivity ratios

Compound	IC_{50} (μM)				Selectivity index[a]	
	pcDHFR	rlDHFR	tgDHFR	mavDHFR	pcDHFR	tgDHFR
1	0.11	0.093	0.1	0.078	0.85	0.93
2	0.85	0.43	0.51	–	0.51	0.84
3	0.49	0.67	1.8	1	1.4	0.37
4	0.49	0.21	0.67	1.0	0.43	0.31
5	5.8	4	6.4	3.6	0.69	0.63
6	1.4	0.13	0.31	0.36	0.09	0.042
7	0.69	0.11	0.17	0.32	0.16	0.65
8	11	19	1.73	1.5	1.7	8.3
9	–	0.17	0.33	0.05	ND	0.52
10	0.38	0.11	0.18	0.056	0.29	0.61
11	1.6	0.73	0.62	0.59	0.46	1.2
12	0.52	0.19	0.13	0.10	0.37	1.5
13	0.27	0.25	0.13	0.053	0.93	1.9
14	1.5	0.35	0.19	0.10	0.23	1.8
15	4.3	0.78	0.33	0.18	0.18	2.4
16	0.98	0.52	0.25	0.1	0.53	2.1
MGN103	0.60	0.39	0.099	–	0.64	3.9
PTX[b]	0.034	0.0044	0.017		0.13	0.26
TMQ[b]	0.042	0.008	0.01		0.19	0.80
TMP[b]	27	121	2.7		4.5	45

[a] Defined as the ratio IC_{50}(rlDHFR)/IC_{50}(pcDHFR) or IC_{50}(rlDHFR)/IC_{50}(tgDHFR).
[b] Data taken from Broughton and Queener (1991), and Chio and Queener (1993).

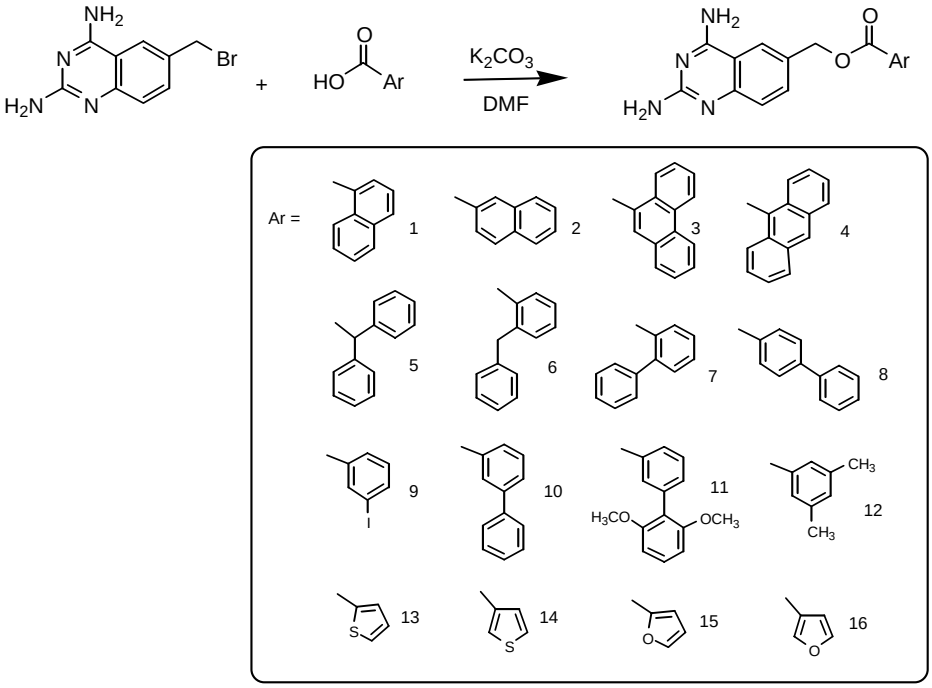

Scheme 1.

3. Results and discussion

3.1. Chemistry

The target compounds **1**–**2**, **5**, **9**, **13**, and **16**, were prepared in DMF by direct displacement of the bromide in 2,4-diamino-6-bromomethylquinazoline (Graffner-Nordberg et al., 2000) using the appropriate carboxylic acid and potassium carbonate as a base (Scheme 1). The syntheses of the esters **3**–**4**, **6**–**8**, **12**, and **14**–**15** were conducted in the Quest 210 organic synthesizer. The Suzuki-couplings with the iodo-compound **9** and phenylboronic acid, or 2,6-dimethoxyphenylboronic acid, providing the esters **10**–**11**, respectively, were conducted in a Smith Synthesizer^{TM} single mode microwave cavity. For the optimization of the appropriate reaction conditions the 'Smith reaction kit' for the Suzuki couplings was used. The catalysts $Pd(PPh_3)_2Cl_2$, $Pd(OAc)_2$, and Hermanns catalyst (*trans*-di-μ-acetobis[2-(di-*o*-tolylphosphino)benzyl]dipalladium(II)), respectively, were examined in the synthesis of **10**. Two different solvent systems were employed [DME/H_2O/EtOH (7:3:2), and DMF, respectively], as well as two inorganic bases (sodium and cesium carbonate). The best results and a full conversion of the iodo-compound **9** was accomplished after 120 s at 140 °C using $Pd(PPh_3)_2Cl_2$ as a pre-catalyst with sodium carbonate as a base in DME/H_2O/EtOH (7:3:2) (Scheme 2). After microwave irradiation for 80 s, at the same reaction temperature, the starting aryl iodide (**9**) still remained as deduced from LC–MS analysis. Yields of 35% (**10**) and 40% (**11**) were isolated. Ester hydrolysis constituted the major side reaction. It is notably that no conversion occurred in the reactions performed in DMF irrespective of the catalyst employed.

3.2. Docking and scoring

A set of structurally diverse esters comprising various aromatic scaffolds were docked and scored using AutoDock 3.0 (Morris et al., 1998). The human reductase (hDHFR) was used in the docking experiments since high resolution 3D structures of inhibitor/enzyme complexes are available. The human reductase exhibits a high homology with rat liver DHFR (Wang et al., 2001). The estimated free energies of binding for the highest ranked structure clusters obtained by

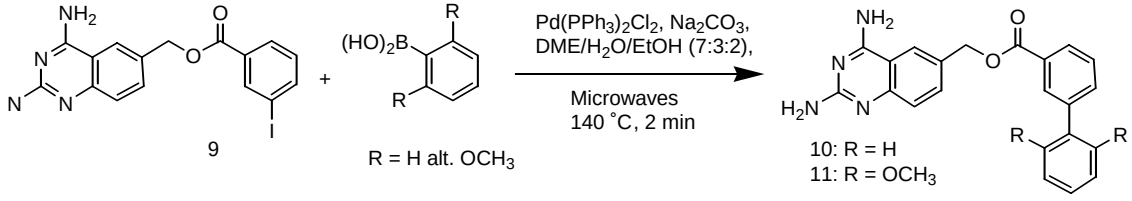

Scheme 2.

Table 2
Calculated free energies of binding obtained by AutoDock compared to experimental IC_{50}-values

Compound	AutoDock[a]				Experimental[a,b]		LIE	
	pc(1DYR)	pc(3CD2)	h(1DLS)	h(1HFR)	pcDHFR	rlDHFR	pc(1DYR)	h(1DLS)
MGN103	−13.1	−12.5	−13.6	−14.2	0.60	0.39		
1	−14.3	−13.8	−15.2	−14.5	**0.11**	**0.09**	−4.5 ± 0.4	−5.3 ± 0.5
2	−14.6	−14.0	−14.9	−14.3	0.85	0.43		
3	**−16.0**	**−15.4**	**−16.1**	**−16.1**	**0.49**	0.67	−7.1±0.3	−7.0 ± 0.7
4	**−15.6**	**−15.6**	**−16.0**	**−15.6**	**0.49**	**0.21**		
5	−15.0	−13.4	−13.7	−14.4	5.8	4		
6	**−15.0**	**−14.3**	**−16.0**	**−15.0**	1.40	**0.13**	−4.9 ± 0.3	−5.9 ± 0.5
7	**−15.1**	**−14.2**	−14.8	−14.8	0.69	**0.11**	−5.2 ± 0.3	−6.0 ± 0.5
8	−14.9	−14.0	**−15.4**	**−14.9**	11	19	−4.6 ± 0.3	−5.3 ± 0.6
10	**−15.6**	**−14.3**	**−15.5**	**−15.1**	**0.38**	**0.11**		
12	−13.8	−13.2	−13.7	−13.4	0.52	0.19		
13	−12.6	−11.9	−13.1	−12.2	**0.27**	0.25		
14	−12.6	−11.9	−13.0	−12.2	1.5	0.35		
15	−12.2	−11.5	−12.9	−11.7	4.3	0.78		
16	−12.4	−11.6	−12.9	−11.7	0.98	0.52		
TMP	−11.2	−10.5	−11.6	−10.6	27	121		

[a] Numbers in bold indicate the five highest ranked compounds in each column.
[b] IC_{50}-values (μM).

AutoDock are summarized in Table 2. As apparent from the table the magnitude of the binding free energies is overestimated (−16 to −11 kcal/mol), which most likely is attributed to an effect from an unbalanced scoring function. However, a comparison of the relative results is still allowed. Although almost all ligands were predicted to bind slightly stronger to hDHFR than to pcDHFR, the scores obtained could not reveal any significant selectivity among the compounds in the series. When comparing the scores obtained from two different DHFR structures from the same species [1HFR (Cody et al., 1998) versus 1DLS (Lewis et al., 1995) modeled from L22Y to wild type, and two of pcDHFR (1DYR (Champness et al., 1994) versus 3CD2 (Cody et al., 1999))] the discrepancy in predicted affinity was in the same magnitude as the difference in affinity when comparing structures from the different species. This implies that the predicted selectivity was smaller than the method allowed estimating. However, the experimental data verified that the selectivity is very low and that a majority of the compounds have slightly higher potency as inhibitors of rlDHFR.

Most compounds that gave the highest scores when docked into the human enzyme were also the best scoring compounds using structures of pcDHFR (Table 2). Moreover, the experimental data obtained for the top five compounds demonstrate that three of them also are among the five most potent inhibitors of rlDHFR. Similarly, for pcDHFR, three out of the five best scoring compounds were among the five most potent inhibitors, as found by experiment. Surprisingly, AutoDock did not rank the most active pcDHFR inhibitor (**1**) very high. When focusing on the lowest ranked compounds the docking and scoring procedure correctly predicted that TMP has the lowest affinity to DHFR among all docked compounds. The potency of compound **5** and **8**, as well as the relatively low inhibitory activity of **6** in the pcDHFR assay, was overestimated by AutoDock using the current protocol. Thus, AutoDock was reasonably good at selecting the most potent DHFR inhibitors, but less successful when picking the least potent ones. A more detailed analysis does not seem meaningful, since both the activity and selectivity of the compounds fall into a very narrow range.

Five of the docked compounds were also selected for studies using the more time consuming linear interaction energy method, which is based on energy averages from molecular dynamics simulations (Åqvist et al., 1994; Marelius et al., 1998c). This method, which does take into account explicit waters and flexibility of the protein, has previously been used to study affinity and selectivity of DHFR inhibitors (Marelius et al., 1998a; Graffner-Nordberg et al., 2000, 2001). The calculated binding free energies obtained from the LIE method also predicted low selectivity of the compounds (hDHFR/pcDHFR). None of the modeled compounds had a calculated difference in binding free energy between hDHFR and pcDHFR that was greater than approximately 1 kcal/mol, in agreement with the experimental data. (A factor of 10 in binding constant corresponds to 1.36 kcal/mol in binding free energy at 298 K.) Considering that the selectivity is very low, of the same size as the errors in the simulations, the predictions by LIE give a qualitatively correct picture. Compound **6** represents the only case where the difference in calculated affinity for pcDHFR and hDHFR was significantly greater than the errors were. Here the measured preference for the human reductase by a factor of 10 is also reproduced, both by LIE and AutoDock. The absolute values of the binding free energies should be interpreted with caution. The constant γ in the LIE equation has not been calibrated to reproduce the experimental binding energies for this protein-ligand system since only

IC_{50}-values and not K_i-values are available (Åqvist and Marelius, 2001). However, as in the case of the results from AutoDock it is still relevant to compare relative affinities.

3.3. Dihydrofolate reductase inhibition

The impact of various linkers connecting the two ring systems has previously been studied thoroughly (Blaney et al., 1984). The lipophilic parts of the ester-based inhibitors **1**–**16** comprise in this study aromatic systems of different sizes and topography. These systems will serve as scaffolds for further synthetic modifications. We first assessed the influence of small methyl groups in the 3- and 5-positions of the phenyl ring of MGN103 (Fig. 1). This modification rendered an inhibitor (**12**) that became slightly more potent than the parent compound and with approximately the same inhibitory effect as the corresponding methoxy-substituted inhibitors (Graffner-Nordberg et al., 2001). Since both alkoxy and methyl groups polarize aromatic systems, we found it relevant to introduce the heterocyclic thiophene and furan nucleus, both with dipoles directed towards the heteroatoms as net effects, as substitutes for the phenyl ring. A comparison of the four heterocycles (**13**–**16**) revealed a dramatic impact on the inhibitory capacity. The high activity of the 2-thienyl derivative (0.27 μM) as compared to the corresponding 2-furyl compound (4.3 μM) is the most striking observation. The fact that a substitution of the phenyl group for a 2-thienyl delivers a twice as active inhibitor while a substitution for the 2-furyl is deleterious is not easy to rationalize. More potent inhibitors than the parent compound MGN103, could also be obtained by an enlargement of the system. Thus, the best inhibitor in the series was obtained by displacement of the phenyl ring for a 1-naphthyl group (**1**). Anchoring of the ester group to a 2-naphthyl group (**2**) resulted in poorer inhibition. Displacements of the 1-naphthyl moiety in **1** for a phenanthrene or an anthracene tricyclic ring system, **3** and **4**, respectively, did not lead to further improvements. It is notable though, that while compound **3** and **4** exhibited the same IC_{50}-values in the pcDHFR assay, the phenanthryl derivative (**3**) was in fact a relatively poor inhibitor of the mammalian reductase [IC_{50}(rlDHFR) = 0.67 μM] and demonstrated a slight preference for the fungal enzyme. Rosowsky et al. (Rosowsky et al., 1999) previously reported the impressive selectivity index of 21 (pcDHFR: 0.21 μM; rlDHFR: 4.4 μM) with a related nitrogen functionalized tricyclic iminostilbene, where a propensity to adopt a puckered orientation was convincingly suggested to account for the high selectivity. Biphenyls were addressed next as scaffolds. A comparison of the impact of phenyl groups attached to the 2, 3 and 4-positions of MGN103, revealed an acceptance for an aromatic ring in the 2-position (**7**) and 3-position (**10**), but not for a substitution in the 4-position (**8**). The 4′-biphenyl compound (**8**) was even less tolerated by rlDHFR and exhibited the highest selectivity index within the series. Introduction of methoxy groups adjacent to the pivotal bond of the 3′-phenyl substituted derivative to restrict rotation was not productive (cf. **10** and **11**), suggesting that a planar system is preferable. The 2′-biphenylic compound (**7**) exhibited only a moderate potency (IC_{50} = 0.69 μM), and was approximately equipotent to MGN103 (IC_{50} = 0.60 μM). However, we felt prompted to further exploit the 2-position, which is in a close proximity to the ester bond of the inhibitor. It was anticipated that proper functionalizations might later allow for control of the rate of enzymatic hydrolysis, an important issue to address in the final fine-tuning of the systems. Displacement of the biphenyl structure for another very common privilege structure, a diphenylmethane group (Hajduk et al., 2000), afforded **6**, that was found to be less active than **7**. Apparently, the insertion of methylene group in **7** to produce a compound with higher flexibility was not well tolerated by pcDHFR. Considering the other diphenylmethyl derivative, compound **5**, this ester is a poor inhibitor of the DHFRs, although still better than the corresponding benzyl ester, lacking one of the two phenyl rings (Graffner-Nordberg et al., 2001).

3.4. Molecular dynamics

Both with regard to the ranking of different inhibitors, as well as the selectivity, there is a reasonable correlation between the results obtained from AutoDock and the LIE method. However, the predicted ranking of the affinities disagrees with experiment in some cases, which may reflect an inexact docking mode. AutoDock docks the flexible ligands into the active site of rigid protein structures and thus, reorientation of side chains upon ligand binding cannot be taken into account. Furthermore, it is also difficult to reproduce the effect of explicit water molecules that may bridge ligand–protein interactions. This problem is of particular relevance in the present study since antifolates bind partly via water bridges to the enzyme (Roth, 1986; Poornima and Dean, 1995; Meiering and Wagner, 1995). The quality of the scoring function is crucial for correct ranking of the docking modes as well as the estimation of the binding free energy. Nevertheless, automated docking is a fast and useful method for screening and affinity predictions on a large set of compounds. Both LIE, and the scoring function used by AutoDock, underestimated the relative affinity of the 4′-biphenyl compound (**8**) to pcDHFR. Both methods also seemed to rank the phenanthryl derivative (**3**) higher than was found by experiment. Furthermore, a relatively high activity of the 1-naphthyl analogue (**1**) was not reproduced. It seems likely that with the present docking procedure there may be a problem in predicting conformational changes that might occur upon binding of large hydrophobic ligands. Even with the more sophisticated molecular dynamics technique it can be difficult to model the correct displacements of amino acid side chains and water molecules if the initially docked structure is non-optimal.

Until high resolution 3D-DHFR complexes with ligands encompassing the ester linkage are available as starting structures for docking programs and MD simulations,

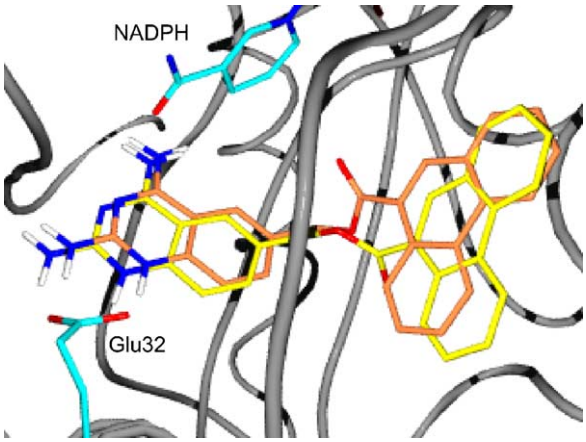

Fig. 3. Compound **3** docked into the active site of pcDHFR (1DYR) using AutoDock. The orientation of the ester moiety is not entirely clear, since the two docked conformations only differ by 0.07 kcal/mol in binding free energy. The conformation where the carbonyl oxygen is pointing upwards is predicted to have the lowest energy.

uncertainties will remain regarding the preferred conformation of the ester group bridging the aromatic parts, as indicated in Fig. 3.

4. Conclusion

Even though the objective of the present program is to achieve a favorable toxicity profile by applying the soft drug concept, it is still highly desirable to optimize the pcDHFR/hDHFR ratio to suppress host toxicity at the site of administration. The most potent of the new ester-based DHFR-inhibitors, the 1-naphthyl derivative (**1**) exhibits an IC_{50}-value of 110 nM, and is less active than trimetrexate with an IC_{50}-value of 42 nM. However, the selectivity index is improved (0.85 versus 0.19 for TMQ). In the group of the most potent inhibitors, the phenanthryl derivative (**3**) exhibits the highest selectivity index, which is still far lower than what is observed with TMP that is used in clinic for treatment of PCP (1.4 versus 4.5 for TMP), in the present assay systems. It is notably though that the new phenanthryl ester exerts a 50 times higher inhibitory activity than TMP. Regarding the computational approaches used for prediction, the calculated results fell into a very narrow range with respect to both affinity and selectivity. The predictions were, with a few exceptions, in qualitatively good agreement with experiments, suggesting that these scoring programs can serve as valuable research tools and guide for further selection of compounds as targets for synthesis.

Acknowledgements

We thank the Swedish Research Council (VR) and the Swedish Foundation for Strategic Research (SSF) for financial support.

References

Allegra, C.J., Chabner, B.A., Tuazon, C.U., Ogata-Agakaki, D., Baird, B., Drake, J.C., Simmons, J.T., Lack, E.E., Shelhamer, J.H., Balis, F., Walker, R., Kovacs, J.A., Lane, H.C., Masur, H., 1987a. Trimetrexate for the treatment of *Pneumocystis carinii* pneumonia in patients with the acquired immunodeficiency syndrome. N. Engl. J. Med. 317, 978–985.

Allegra, C.J., Kovacs, J.A., Drake, J.C., Swan, J.C., Chabner, B.A., Masur, H., 1987b. Activity of antifolates against *Pneumocystis carinii* dihydrofolate reductase and identification of a potent new agent. J. Exp. Med. 165, 926–931.

Anonymous, 1994. News. FDA approves trimetrexate as a second line therapy for *Pneumocystis carinii* pneumonia. Am. J. Hosp. Pharm. 51, 591–592.

Åqvist, J., Marelius, J., 2001 The linear interaction energy method for predicting ligand binding free energies. In: Reddy, M.R., Erion, M.D. (Eds.), Free Energy Calculations in Rational Drug Design. Kluwer Academic Publishers, Dordrecht.

Åqvist, J., Medina, C., Samuelsson, J.E., 1994. A new method for predicting binding affinity in computer-aided drug design. Protein Eng. 7, 385–391.

Arozullah, A.M., Yarnold, P.R., Weinstein, R.A., Nwadiaro, N., McIlraith, T.B., Chmiel, J.S., Sipler, A.M., Chan, C., Goetz, M.B., Schwartz, D.N., Bennett, C.L., 2000. A new preadmission staging system for predicting inpatient mortality from HIV-associated *Pneumocystis carinii* pneumonia in the early highly active antiretroviral therapy (HAART) era. Am. J. Respir. Crit. Care Med. 161, 1081–1086.

Bertino, J.R., Sawacki, W.L., Moroson, B.A., Cashmore, A.R., Elslager, E.F., 1979. 2,4-Diamino-5-methyl-6-[(2,4,5-trimethoxyanilino)-methyl]quinazoline (TMQ), a potent non-classical folate antagonist inhibitor-I. Biochem. Pharmacol. 28, 1983–1987.

Blaney, J.M., Hansch, C., Silipo, C., Vittoria, A., 1984. Structure-activity relationships of dihydrofolate reductase inhibitors. Chem. Rev. 84, 333–407.

Bodor, N., Buchwald, P., 2000. Soft drug design: general principles and recent applications. Med. Res. Rev. 20, 58–101.

Broughton, M.C., Queener, S.F., 1991. *Pneumocystis carinii* dihydrofolate reductase used to screen potential antipneumocystis drugs. Antimicrob. Agents Chemother. 35, 1348–1355.

Champness, J.N., Achari, A., Ballantine, S.P., Bryant, P.K., Delves, C.J., Stammers, D.K., 1994. The structure of *Pneumocystis Carinii* dihydrofolate reductase to 1.9 Å resolution. Structure 2, 915–924.

Chio, L.-C., Queener, S.F., 1993. Identification of highly potent and selective inhibitors of *Toxoplasma gondii* dihydrofolate reductase. Antimicrob. Agents Chemother. 37, 1914–1923.

Clissold, S.P., Heel, R.C., 1984. Budesonide: a preliminary review of its pharmacodynamic properties and therapeutic efficacy in asthma and rhinitis. Drugs 28, 485–518.

Cody, V., Galitsky, N., Luft, J.R., Pangborn, W., Blakley, R.L., Gangjee, A., 1998. Comparison of ternary crystal complexes of F31 variants of human dihydrofolate reductase with NADPH and a classical antitumor furopyrimidine. Anticancer Drug Des. 13, 307–315.

Cody, V., Galitsky, N., Rak, D., Luft, J.R., Pangborn, W., Queener, S.F., 1999. Ligand-induced conformational changes in the crystal structures of *Pneumocystis carinii* dihydrofolate reductase complexes with folate and $NADP^+$. Biochemistry 38, 4303–4312.

Duch, D.S., Edelstein, M.P., Bowers, S.W., Nichol, C.A., 1982. Biochemical and chemotherapeutic studies on 2,4-diamino-6-(2,5-dimethoxybenzyl)-5-methylpyrido[2,3-*d*]pyrimidine (BW301U), A novel lipid-soluble inhibitor of dihydrofolate reductase. Cancer Res. 42, 3987–3994.

Elslager, E.F., Davoll, J., 1974. Synthesis of fused pyrimidines as folate antagonists. In: Castle, R.N., Townsend, L.B. (Eds.), Lectures in Heterocyclic Chemistry. Hetero Corp., Orem, UT.

Elslager, E.F., Johnson, J.L., Werbel, L.M., 1983. Folate antagonists. 20. synthesis, antitumor, and antimalarial properties of trimetrexate and related 6-[(phenylamino)methyl]-2,4-quinazolindiamines. J. Med. Chem. 26, 1753–1760.

Falloon, J., Allegra, C.J., Kovacs, J., O'Neill, D., Ogata-Arakaki, D., Feuerstein, I., Polis, M., Davey, R., Lane, H.C., LaFon, S., Rogers, M., Zunich, K., Turlo, J., Tuazon, C., Parenti, D., Simon, G., Masur, H., 1990. Piritrexim with leucovorin for the treatment of *Pneumocystis* Pneumonia (PCP) in AIDS patients. Clin. Res. 38, 361A.

Fischl, M.A., Dickinson, G.M., La Voie, L., 1988. Safety and efficiency of sulfamethoxazole and trimethoprim chemoprophylaxis for *Pneumocystis carinii* pneumonia in AIDS. J. Am. Med. Assoc. 105, 45–48.

Glatt, A.E., Chirgwin, K., 1990. *Pneumocystis carinii* pneumonia in human immunodeficiency virus-infected patients. Arch. Intern. Med. 150, 271–279.

Golden, J.A., Chernoff, D., Hollander, H., Feigal, D., Conte, J.E., 1989. Prevention of *Pneumocystis carinii* by inhaled pentamidine. Lancet 1, 654–657.

Gordin, F.M., Simon, G.L., Wofsy, C.B., Mills, J., 1984. Adverse reactions to trimethoprim-sulfamethoxazole in patients with the acquired immunodeficiency syndrome. Ann. Intern. Med. 100, 495–499.

Graffner-Nordberg, M., Kolmodin, K., Åqvist, J., Queener, S.F., Hallberg, A., 2001. Design, synthesis, computational prediction and biological evaluation of ester soft drugs as inhibitors of dihydrofolate reductase from *Pneumocystis carinii*. J. Med. Chem. 44, 2391–2402.

Graffner-Nordberg, M., Marelius, J., Ohlsson, S., Persson, Å., Swedberg, G., Andersson, P., Andersson, S.E., Åqvist, J., Hallberg, A., 2000. Computational predictions of binding affinities to dihydrofolate reductase: synthesis and biological evaluation of methotrexate Analogues. J. Med. Chem. 43, 3852–3861.

Grivsky, E.M., Lee, S., Sigel, C.W., Duch, D.S., Nichol, C.A., 1980. Synthesis and antitumor activity of 2,4-diamino-6-(2,5-dimethoxybenzyl)-5-methylpyrido[2,3-d]pyrimidine. J. Med. Chem. 23, 327–329.

Hajduk, P.J., Bures, M., Praestgaard, J., Fesik, S.W., 2000. Privileged molecules for protein binding identified from NMR-based screening. J. Med. Chem. 43, 3443–3447.

Hirschel, B., Lazzarin, A., Chopard, P., 1991. A controlled study of inhaled pentamidine for primary prevention of *Pneumocystis carinii* pneumonia. N. Engl. J. Med. 324, 1079–1083.

Johansson, S.-Å., Andersson, K.-E., Brattsand, R., Gruvstad, E., Hedner, P., 1982. Topical and systemic glucocorticoid potencies of budesonide and beclomethasone dipropionate in man. Eur. J. Clin. Pharmacol. 22, 523–529.

Kaplan, J.E., Hanson, D., Dworkin, M.S., Frederick, T., Bertolli, J., Lindegren, M.L., Holmberg, S., Jones, J.L., 2000. Epidemiology of human immunodeficiency virus-associated opportunistic infections in the united states in the era of highly active antiretroviral therapy. Clin. Infect. Dis. 30 (Suppl. 1), S5–S14.

Kovacs, J.A., Allegra, C.A., Swan, J.C., Drake, J.C., Parillo, J.E., Chabner, B.A., Masur, H., 1988. Potent antipneumocystis and antitoxoplasma activities of piritrexim, a lipid-soluble antifolate. Antimicrob. Agents Chemother. 32, 430–433.

Kovacs, J.A., Hiemenz, J.W., Macher, A.M., Stover, D., Murray, H.W., Shelhamer, J., Lane, H.C., Urmacher, C., Honig, C., Longo, D.L., Parker, M.M., Natanson, C., Parillo, J.E., Fauci, A.S., Pizzo, P.A., Masur, H., 1984. *Pneumocystis carinii* pneumonia: a comparison between patients with the acquired immunodeficiency syndrome and patients with other immunodeficiencies. Ann. Intern. Med. 100, 663–671.

Lee, F.S., Warshel, A., 1992. A local reaction field method for fast evaluation of long-range electrostatic interactions in molecular simulations. J. Chem. Phys. 97, 3100–3107.

Leoung, G.S., Feigal, D.W., Montgomery, A.B., Corkery, K., Wardlaw, L., Adams, M., Busch, D., Cordon, S., Jacobson, M.A., Volberding, P.A., Abrams, D., 1990. Aerosolized pentamidine for prophylaxis against *Pneumocystis carinii* pneumonia. N. Engl. J. Med. 323, 769–775.

Lewis, W.S., Cody, V., Galitsky, N., Luft, J.R., Pangborn, W., Chunduru, S.K., Spencer, H.T., Appleman, J.R., Blakley, R.L., 1995. Methotrexate-resistant variants of human dihydrofolate reductase with substitutions of leucine 22: kinetics, crystallography, and potential as selectable markers. J. Biol. Chem. 270, 5057–5064.

Lin, J.T., Cashmore, A.R., Baker, M., Dreyer, R.N., Ernstoff, M., Marsh, J.C., Bertino, J.R., Whitfield, L.R., Delap, R., Grillo-Lopez, A., 1987. Phase I studies with trimetrexate: clinical pharmacology, analytical methodology, and pharmacokinetics. Cancer Res. 47, 609–616.

Marelius, J., Graffner-Nordberg, M., Hansson, T., Hallberg, A., Åqvist, J., 1998a. Computation of affinity and selectivity: binding of 2,4-diaminopteridine and 2,4-diaminoquinazoline inhibitors to dihydrofolate reductases. J. Comput. Aided Mol. Des. 12, 119–131.

Marelius, J., Hansson, T., Åqvist, J., 1998c. Calculation of ligand binding free energies from molecular dynamics simulations. Int. J. Quant. Chem. 69, 77–88.

Marelius, J., Kolmodin, K., Feierberg, I., Åqvist, J., 1998b. Q: an MD program for free energy calculations and empirical valence bond simulations in biomolecular systems. J. Mol. Graph. Model. 16, 213–225.

Masur, H., 1992. Prevention and treatment of *Pneumocystis* pneumonia. N. Engl. J. Med. 327, 1853–1860.

Masur, H., Polis, M.A., Tuazon, C.V., Ogota, A.D., Kovacs, J.A., Katz, D., Hilt, D., Simmons, T., Feuerstein, I., Lundgren, B., Lane, H.C., Chabner, B.A., Allegra, C.J., 1993. Salvage trial of trimetrexate-leucovorin for the treatment of cerebral toxoplasmosis. J. Infect. Dis. 167, 1422–1426.

McKenzie, R., Travis, W.D., Dolan, S.A., 1991. The causes of death in patients with human immunodeficiency virus infections: a clinical and pathological study with emphasis on the role of pulmonary diseases. Medicine (Baltimore) 70, 326–343.

Meiering, E.M., Wagner, G., 1995. Detection of long-lived bound water molecules in complex of human dihydrofolate reductase with methotrexate and NADPH. J. Mol. Biol. 247, 294–308.

Miller, R.F., Mitchell, D.M., 1995. AIDS and the lung. Update 1995: 1 *Pneumocystis carinii* pneumonia. Thorax 50, 191–200.

Mills, J., 1986. *Pneumocystis carinii* and *Toxoplasma gondii* infections in patients with AIDS. Rev. Infect. Dis. 8, 1001–1011.

Monk, J.P., Benfield, P., 1990. Inhaled pentamidine. An overview of its pharmacological properties and a review of its therapeutic use in pneumocystis carinii pneumonia. Drugs 39, 741–756.

Morris, G.M., Goodsell, D.S., Halliday, R.S., Huey, R., Hart, W.E., Belewm, R.K., Olson, A.J., 1998. Automated docking using a lamarckian genetic algorithm and empirical binding free energy function. J. Comput. Chem. 19, 1639–1662.

Pearson, R.D., Hewlett, E.L., 1985. Pentamidine for the treatment of *Pneumocystis carinii* pneumonia and other protozoal diseases. Ann. Intern. Med. 103, 782–786.

Poornima, C.S., Dean, P.M., 1995. Hydration in drug design. 3. Conserved water molecules at the ligand-binding sites of homologous proteins. J. Comput. Aided Mol. Des. 9, 521–531.

Rosowsky, A., Cody, V., Galitsky, N., Fu, H., Papoulis, A.T., Queener, S.F., 1999. Structure-based design of selective inhibitors of dihydrofolate reductase: synthesis and antiparasitic activity of 2,4-diaminopteridine analogues with a bridged diarylamine side chain. J. Med. Chem. 42, 4853–4860.

Roth, B., 1986. Design of dihydrofolate reductase inhibitors from X-ray crystal structures. Fed. Proc. 45, 2765–2772.

Roudier, C., Caumes, E., Rogeauz, O., Bricaire, F., Gentilini, M., 1994. Adverse cutanous reactions to trimethoprim-sulfamethoxazole in patients with the acquired immunodeficiency syndrome and *Pneumocystis carinii* pneumonia. Arch. Dermatol. 30, 1383–1386.

Sattler, F.R., Allegra, C.J., Verdegem, T.D., 1990. Trimetrexate-leucoverin dosage evaluation study for the treatment of *Pneumocystis carinii* pneumonia. J. Infect. Dis. 161, 91–96.

Schliep, T.C., Yarrish, R.L., 1999. *Pneumocystis carinii* pneumonia. Semin. Respir. Infect. 14, 333–343.

van Gunsteren, W.F., Berendsen, H.J.C., 1987. Groningen Molecular Simulation (GROMOS) Library Manual, Biomos B.V., Groningen.

Walker, R.E., Masur H., 1994. Current regimens of therapy and prophylaxis. In: Walzer, P.D. (Ed.), *Pneumocystis carinii* Pneumonia. Marcel Dekker, New York, pp. 439–466.

Wang, Y., Bruenn, J.A., Queener, S.F., Cody, V., 2001. Isolation of rat dihydrofolate reductase gene and characterization of recombinant enzyme. Antimicrob. Agents Chemother. 45, 2517–2523.

Weir, E.C., Cashmore, A.R., Dreyer, R.N., Graham, M.L., Hsiao, N., Moroson, B.A., Sawacki, W.L., Bertino, J.R., 1982. Pharmacology and toxicity of a potent "nonclassical" 2,4-diamino quinazoline folate antagonist, trimetrexate, in normal dogs. Cancer Res. 42, 1696–1702.